



LOCATION MAPPING OF HYDROTHERMAL ALTERATION USING LANDSAT 8 DATA: A CASE OF STUDY IN PRESTEA HUNI VALLEY DISTRICT, GHANA

 Ibrahim Abdul Sulemana^{1*}

 Jonathan Quaye-Ballard²

 Clement Ntori³

 Alfred Awotwi⁴

 Oladunjoye Michael Adeyinka⁵

 Thomas Moore Okrah⁶

 Abena Asare-Ansah⁷

^{1,2}Pan African University Institute of Earth and Life Science Including Agriculture (PAULESI), University of Ibadan, Nigeria.

³Email: Kalibradus26@gmail.com Tel: +233544996813

⁴Email: Clement.ntori@gmail.com Tel: +233240172113

^{2,6,7} Department of Geomatic Engineering, Kwame Nkrumah University of Science and Technology (KNUST), Kumasi, Ghana.

⁵Email: quayeballard@yahoo.com Tel: +233277474073

⁶Email: Otom789@gmail.com Tel: +233245264730

⁷Email: asareansah@gmail.com Tel: +233541173762

⁴Department of Earth and Environmental Science, University for Development Studies (UDS), Navrongo, Ghana.

⁵Email: Awor73@yahoo.com Tel: +233242268905

⁶Department of Geology, University of Ibadan (UI), Ibadan, Nigeria.

⁷Email: ma.oladunjoye@yahoo.com Tel: +2348163265217



(+ Corresponding author)

ABSTRACT

Article History

Received: 30 October 2019

Revised: 29 November 2019

Accepted: 2 January 2020

Published: 13 February 2020

Keywords

Principle component analysis

PCA

Band Ratio

Hydrothermal alteration

Hydroxyl minerals

Mineralization

Ghana.

Utilization of multispectral satellite images is an excellent approach in the reconnaissance stage of gold prospecting due to its high effectiveness and low cost. This research used Landsat 8 Remote Sensing data and Geographical Information System to identify, delineate and map hydrothermal alteration zone relating to gold pattern mineralization in Prestea Huni Valley District in the Western Region of Ghana. Principle Component Analysis (PCA), three band combinations, spectral rationing and Crosta techniques are used in this study. For three band combinations, bands 5, 4, 3 and 5, 6, 7 are used to map location of hydrothermal alterations. Band ratios (7/5 and 6/7), (6/5) and (4/2) are used to identify presence of clay, ferrous and iron oxide minerals respectively. Sabin's ratio 4/2, 6/7 and 6/5, Kaufmann ratio 7/5, 5/4 and 6/7, and 4/2, 6/7 and 5 are used to identify vegetation, outcrop and hydrothermal alterations respectively. Crosta and PCA techniques were used to suppress the interference of vegetation in delineating the alteration zones. Results revealed that the three band combinations and spectral ratioing clearly depicts hydrothermal deposit of ferrous minerals, clay and iron oxide minerals. PCA identifies presence of iron-oxide and hydroxyl minerals as bright pixels. The first three high order principal components (PC1, PC2 and PC3) of input spectral bands gave more than 98% of the spectral information. Thus, the results from satellite images an effective and efficient way of mapping hydrothermal alteration zones at regional scale.

Contribution/Originality: This is one of the very few studies which have investigated to identify hydrothermally alteration relating to gold mineralization. The study documents how Satellite data and Remote Sensing and Geographical Information System techniques can be used to delineate hydrothermal alterations at regional scale at a reduced cost.

1. INTRODUCTION

Remote Sensing (RS) has proved to be an important tool tracing mineral deposits by distinguishing processes of mineralization through spectral anomalies (Rajesh, 2004; Van der Meer *et al.*, 2012). RS is a powerful technique in identifying hydrothermally altered rocks, structures, lineaments, oxidation products, morphology, lithological units, vegetation anomalies and other valuable information to geologists (Goetz *et al.*, 1982; Goetz, 2009). It is broadly acknowledged that hydrothermal alteration plays an important role in mineral prospecting. The necessary dispersal of alteration zones around the limited borders of an ore body helps narrow down the exploration events into smaller targets (Masoumi *et al.*, 2017). Hydrothermal mineralization alteration is a process which alters the mineralogy and chemistry of the host rocks resulting in creating mineral assemblages which differ according to the setting, degree and time of the alteration processes (Mia and Fujimitsu, 2012; Sadiya *et al.*, 2014). Usually, hydrothermal alteration processes lead to the formation of clay and other silicate minerals including kaolinite, sericite, illite, quartz, chlorite, epidote, and calcite (Ranjbar *et al.*, 2004).

Spectral ratioing (arithmetic operations) and three band combinations of remotely sensed data can detect the above-mentioned minerals and discover buried deposits (Masoumi *et al.*, 2017). Band ratioing have been used by different authors to examine and interpreted remotely sensed data to map hydrothermally alteration relating to minerals deposit patterns. For example, Gad and Kusky (2007) used ASTER band ratios 4/7, 4/6 and 4/10 to map the granite and metamorphic belt of the Wadi Kid area of Sinai, Egypt. Pour *et al.* (2017) applied qualitative image processing procedures such as colour composites, band ratios and Principal Components Analysis (PCA) on ASTER and Landsat-8 bands to map lithological and alteration minerals in poorly exposed lithologies in north-eastern Graham Land, Antarctic Peninsula. Sadiya *et al.* (2014) used band ratioing, PCA and crosta technique to map and detect minerals in Bwari Area Council, Abuja Nigeria. According to Sadiya *et al.* (2014) band ratios 3/1, 4/5 – 4/3 and 5/7 suggests the presence of ferric iron minerals, hydroxyl minerals and clay mineralization respectively. Also, band ratios 3/1, 4/5 – 4/3 and a sum of the band ratios (3/1, 4/5 – 4/3) displayed as RGB enhanced the location of mineral deposits. Applications of remotely sensed satellite data are widely used and unique in mapping of different lithologies, mineral resources, ore deposits and minerals of alteration zone in many types of deposits, such as porphyry copper deposits (Alimohammadi *et al.*, 2015; Abuzied *et al.*, 2016). Long term Landsat data has made possible in the advancement of using the satellite images in geological application. The development in the image processing methods which can be used to improve the satellite images and show the spectral appearances of required features on the ground (Pour and Hashim, 2014). Landsat TM data, both TM5 and TM7 are among the most utilized satellite multispectral remote sensing data in mineral investigation (Mshiu *et al.*, 2015). The datasets are utilized to find target zones in the reconnaissance phases of investigation (example (Kruse *et al.*, 2002; Crosta *et al.*, 2003)). They are equipped for distinguishing the territories rich in Fe-minerals and earth ± carbonate ± sulfate minerals. Landsat 8 data can detect the altered rocks and ferrous minerals through the Operational Land Imager (OLI) part of the image due to the absorption and reflectance characteristics of these rocks which appear in this range (Abhary and Hassani, 2016). When it comes to silicate the two additional thermal bands have the ability to detect the reflectance characteristic for it in their range (Dehnavi *et al.*, 2010). Landsat-8 OLI/TIRS data can be utilized to monitor variety of earth-based and atmospheric occurrence, including rural observing; topographical mapping; evapotranspiration; cloud location and examination; mapping heat motions from urban communities; checking air quality; checking volcanic movement; biomass consuming; mechanical warm contamination in the environment, streams and lakes; checking/following material transport in lakes and seaside locales; finding insect breeding zones and applications that will ultimately arise later as a result of global warming and climate change (Pour and Hashim, 2014). In Ghana, there has been exceptionally small research in utilizing remote sensing techniques to identify mineral deposits. One of the few carried out was (Kwang *et al.*, 2014) they applied remote sensing (RS) and geographical information system techniques (GIS) to map gold potential areas at Birim North District in the Eastern Region of Ghana. However, a remote sensing study has barely been carried out in the

Prestea Huni Valley district to identify hydrothermally alteration relating to gold mineralization. The aim of this study is to use remote sensing and GIS techniques to detect and map location of hydrothermal alteration relating to gold pattern mineralization in the Prestea Huni Valley district as a means of producing a mineral deposit database for Ghana. This study offers detailed understanding and effective way of prospecting for gold, which is an economic livelihood of the economy of Ghana, critical for effective planning, at the Prestea Huni Valley District of Ghana to confirm sustainable accessibility of gold for present and future generation.

2. MATERIALS AND METHODS

2.1. Study Area

The Prestea Huni Valley District lies approximately on latitude 5° 20'N and 5° 40'N and between longitude 1° 50'W and 2° 10'W. The Prestea/Huni-Valley District Assembly is one of the recently made Districts in the western area. It was cut out from the then Wassa West District Assembly in 2004 and has its central station at Bogoso, which is a mining town arranged around 33 kilometers north of Tarkwa. Prestea/Huni-Valley District Assembly imparts limits on the north west to Wassa Amenfi Central District, on the south east with Wassa East District, on the south west with Axim Municipal Assembly, on the south with Tarkwa-Nsuaem Municipal Assembly and toward the north by Wassa Amenfi East District Assembly (MLGRD, 2006). The district lies within the South Western Equatorial Zone (Oduro, 2011).

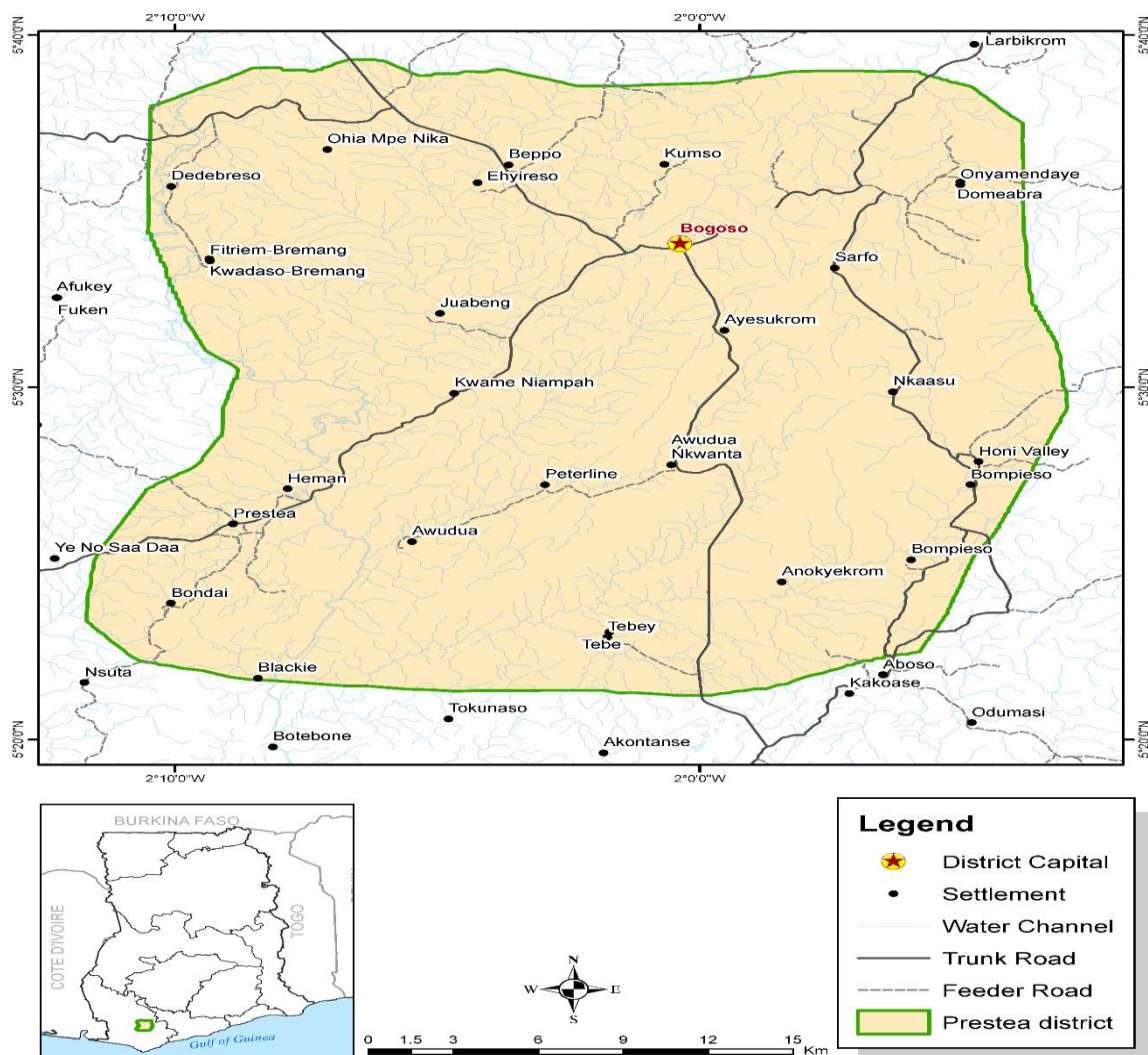


Figure-1. Location of the study area.

2.1.1. Geology of the Study Area

The geology of southwestern Ghana is dominated by the Birimian Supergroup, which is comprised of Proterozoic sedimentary and volcanic rocks. These units are intensely deformed by faulting and folding activities and were later intruded by various granitoid intrusions. Overlying the Birimian unit is a less deformed coarse clastic sediments of the Tarkwa group which is thought to be erosional products of the Birimian Supergroup and Belt type granitoids that were deposited in long narrow intermontane grabens, which formed as the result of localized rifting in the Birimian metavolcanic belts (Leube *et al.*, 1990). All these formational events took place during the Eburnean orogeny which affected the whole of Ghana spanning from 2,080 to 2,240Ma (Kesse, 1985). Rocks of the Tarkwaian Group are characteristically highly magnetic and can be identified easily on aeromagnetic images (Griffis, 1998).

The Prestea concession falls within the southern part of the Ashanti greenstone belt which host world class gold mineral deposits; and it's characterized by a large number of gold deposits including active and mines like Anglogold Ashanti, Golden Star Resources at Prestea and Bogosso and Gold Fields at Tarkwa and Damang (Kuma *et al.*, 2010). The geology of the Prestea concession is grouped into three main rock-structural units which are separated by a westward steeply dipping fault. These structural assemblages are; the Tarkwaian litho-structural units, the tectonic structural units made up of sheared graphitic sediments and volcanic flows and undeformed sedimentary units of the Kumasi basin. Both rocks and Mineralization are structurally controlled and conforms to the regional NNE to NE tectonic corridors which affected southwestern Ghana (Griffis *et al.*, 2002). The style of gold mineralization occurs in variable forms within the belt which include gold associated with quartz veins and disseminated types, gold bearing pebble conglomerate which is typical of the Tarkwaian group, alluvial and oxide deposits (Kuma *et al.*, 2010).

The eastern part of the concession is made up of the Tarkwaian litho-structural units which comprise of sandstones, pebbly sandstone, and conglomerates. The quartz pebble conglomerates are by far the most important member of the group because of its gold mineralizing potential. The deformational activities have resulted in the formation of another litho-structural units which overlies the Tarkwaian sediments called the tectonic breccia. These are formed in areas which share close contact with the Kumasi sedimentary basin. Various forms of alteration patterns are used to separate one volcanic unit from the other. Weakly altered mafic volcanic rocks are characterized by distal chlorite/calcite alterations patterns while strongly altered mafic volcanic rocks which are generally located at the main Reef Fault are characterized by silica/sericite/Fe-Mg carbonates alteration patterns. Finally, within the tectonic assemblage, very distinctly, the volcanic lenses are seen to intercalate with the sheared graphitic sedimentary horizons which represents sheared and brecciated sequences of siltstone, mudstone and greywacke units affected by pervasive graphitic alteration (Griffis *et al.*, 2002). The primary features within these units are generally overprinted and destroyed by deformational activities even though primary beds are locally preserved. All the major lithologies are illustrated in Figure 2.

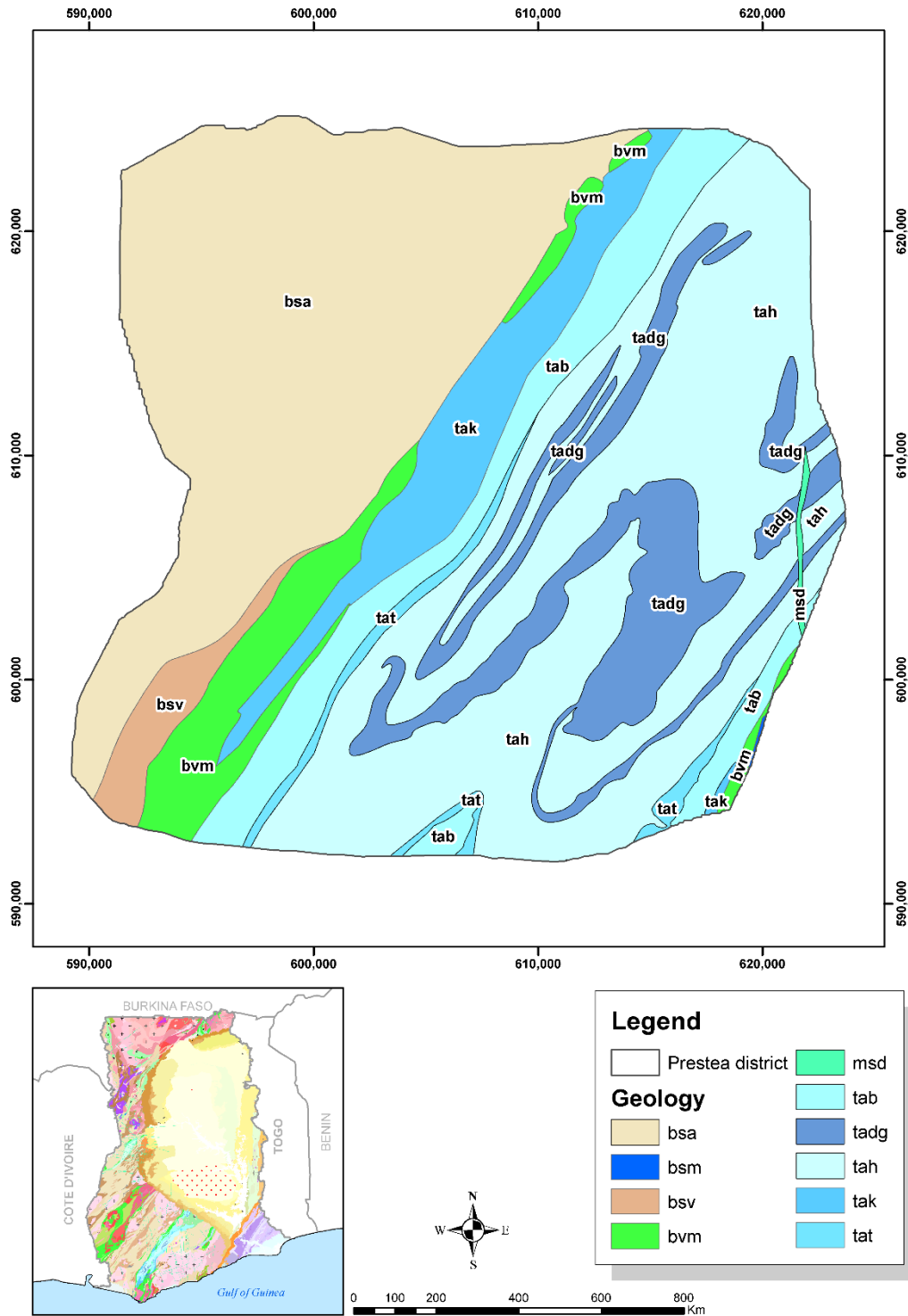


Figure-2. Showing major rock types in the study area.

Source: Kesse (1985).

2.2. Data

The RS image used is Landsat 8. It was downloaded from Google Earth Engine Platform (<https://code.earthengine.google.com/2854ac10f2cc8be21ebdb5918a86d69b>). This image (cloud free) was captured on 15 of February 2016 according to Google Earth Engine Platform. Geological Map was obtained from the Geological Survey Department at a scale of 1:1000000.

2.3. Method

2.3.1. Image Processing Techniques

Spectral characteristics of the study area in term of mapping hydrothermal alteration zones were presented using Remote Sensing techniques. Sub-setting and stacking image processing were performed on the Landsat 8 image to obtain the boundary image of the study area. Image enhancement method such as colour composite, band rationing and principal component analysis were executed on the image of the study area to map location of hydrothermal alteration relating to gold mineralization in the study area.

2.3.2. Three Band Combinations

Three band combinations (false colour composite) is useful for mineral and rock discrimination and infer possible alterations centered in colour intensity disparities. A composite with the visible bands of the spectrum that correspond to red, green and blue is called a true colour composite. When a composite is created with non-visible bands it is called a false colour composite image. Different false colour composites were generated using bands 5, 4, 3 and 5, 6, 7 for the purpose of mapping location of alteration mapping.

2.3.3. Spectral Ratioing (Band Ratioing)

Spectral ratioing or band ratioing is a multispectral image processing method that involves the arithmetic division of one spectral band by another. This arithmetic division results in the ratio of spectral reflectance measured in the one spectral band to the spectral reflectance measured in another spectral band. Spectral ratioing transforms the data thereby minimizing the effects of such environmental conditions (Jensen and Lulla, 1987). ArcGIS software was used to performed band ratios using various bands in Landsat 8 for enhancement of spectral signatures for alteration minerals. Clay minerals alterations were highlighted using the Landsat 8 band ratios 7/5 and 6/7. Landsat 8 band ratio 4/2 was used to discriminate alteration patterns for iron minerals. Landsat 8 band ratio 6/5 was used to highlights alteration patterns for ferrous minerals. Colour combination of band ratios 4/2, 6/7 and 5 were used for the detection of hydrothermal zones. For instance Sabins (1999) and Kaufmann (1988) used band ratios for discriminating between altered rocks, vegetation and rock types which yielded significant results.

2.3.4. Principal Component Analysis (PCA)

PCA is a multivariate statistical strategy that examines the Eigenvector loadings of a multispectral satellite data to determine the unique spectral reaction of distinctive minerals and rocks contained in the image called Crosta technique (Crosta *et al.*, 2003; Mia and Fujimitsu, 2012). PCA is normally utilized for distinguishing and mapping the dispersion of alteration in metallogenic regions (Nouri *et al.*, 2012). The panchromatic image is histogram coordinated to the first PC. It then substitutes the selected component and a reverse PC transform takes the merged dataset back into the original multispectral feature space (Chavez *et al.*, 1991). By applying PCA a new data set with lesser variables is formed (Lillesand *et al.*, 2000). PC1 is generally the weighted average of all data and represents albedo and topographic effects found in the scene (Ranjbar *et al.*, 2004). Sabins (1999) effectively adopted an approach where PCA of band sets 1347 and 1547 were processed individually to determine the occurrence of iron-oxide and hydroxyl-rich minerals. The method guarantees the undesirable signals from materials such as vegetation are isolated from geological/ mineralogical target materials and collect them in a separate principal component (PC). Crosta strategy does not require much consideration on pretreatments to suppress signals from vegetation since the undesirable signals will be collected in other PCs, different from the PC conveying target signals (Mshiu *et al.*, 2015). It is by and large acknowledged that the first three high order principal components (PC1, PC2 and PC3) of input spectral bands gave more than 99% of the spectral information, while lower order components usually contain low signal-to-noise ratios (Amer *et al.*, 2010).

3. RESULTS

3.1. Colour Composite

Using false colour composite, hydrothermal zones with mineral spectral signatures near infrared (IR) to mid-infrared can be detected using ETM+ (Jensen, 2005). In Figure 3, red represents vegetation, black represents water and the greyish colour represents rock or soil. Vegetated areas appear in red, outcrops in light blue and water in black and hydrothermal altered rocks can be identified as blue Figure 4.

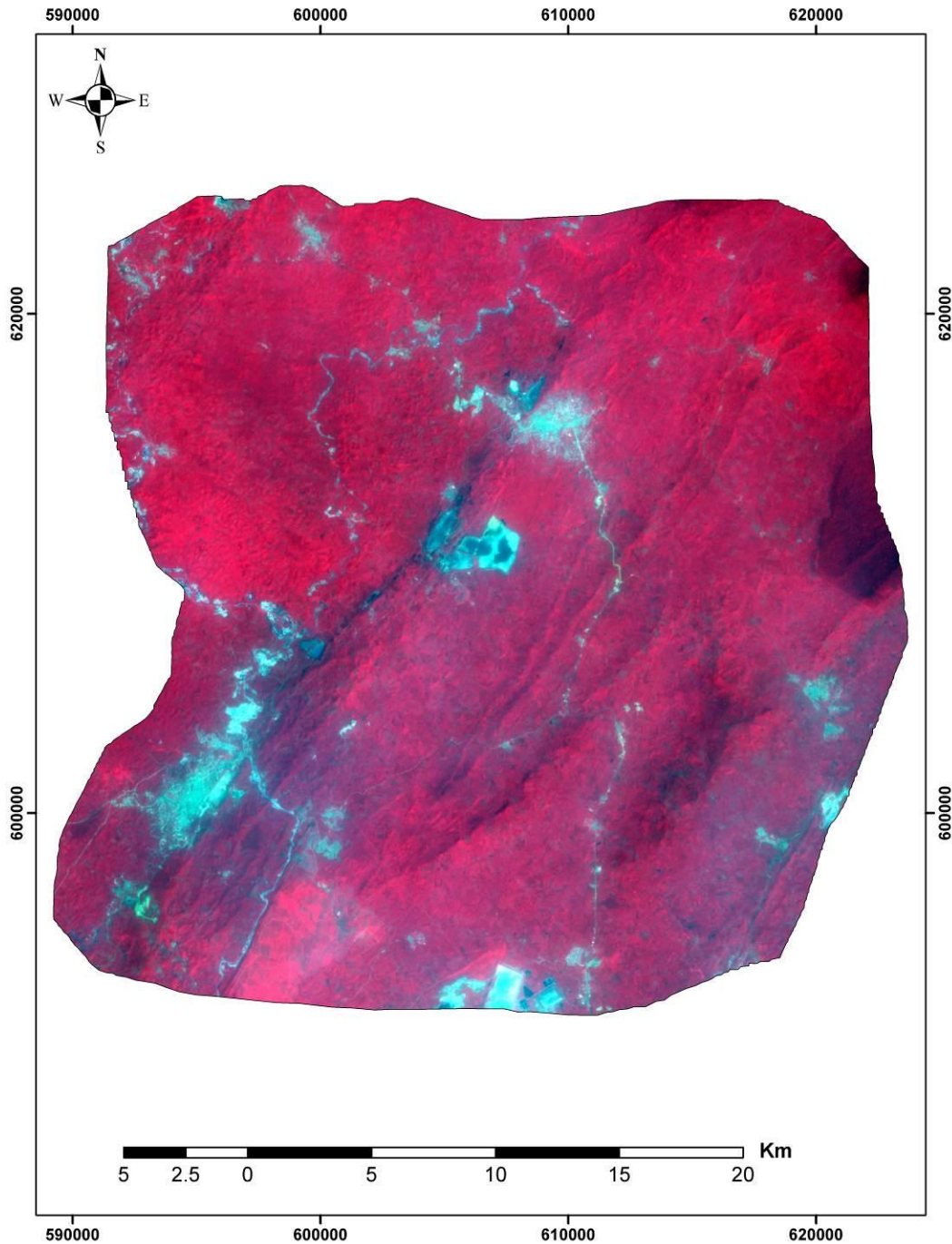


Figure-3. False colour composite Bands 5, 4, 3, in the study area.

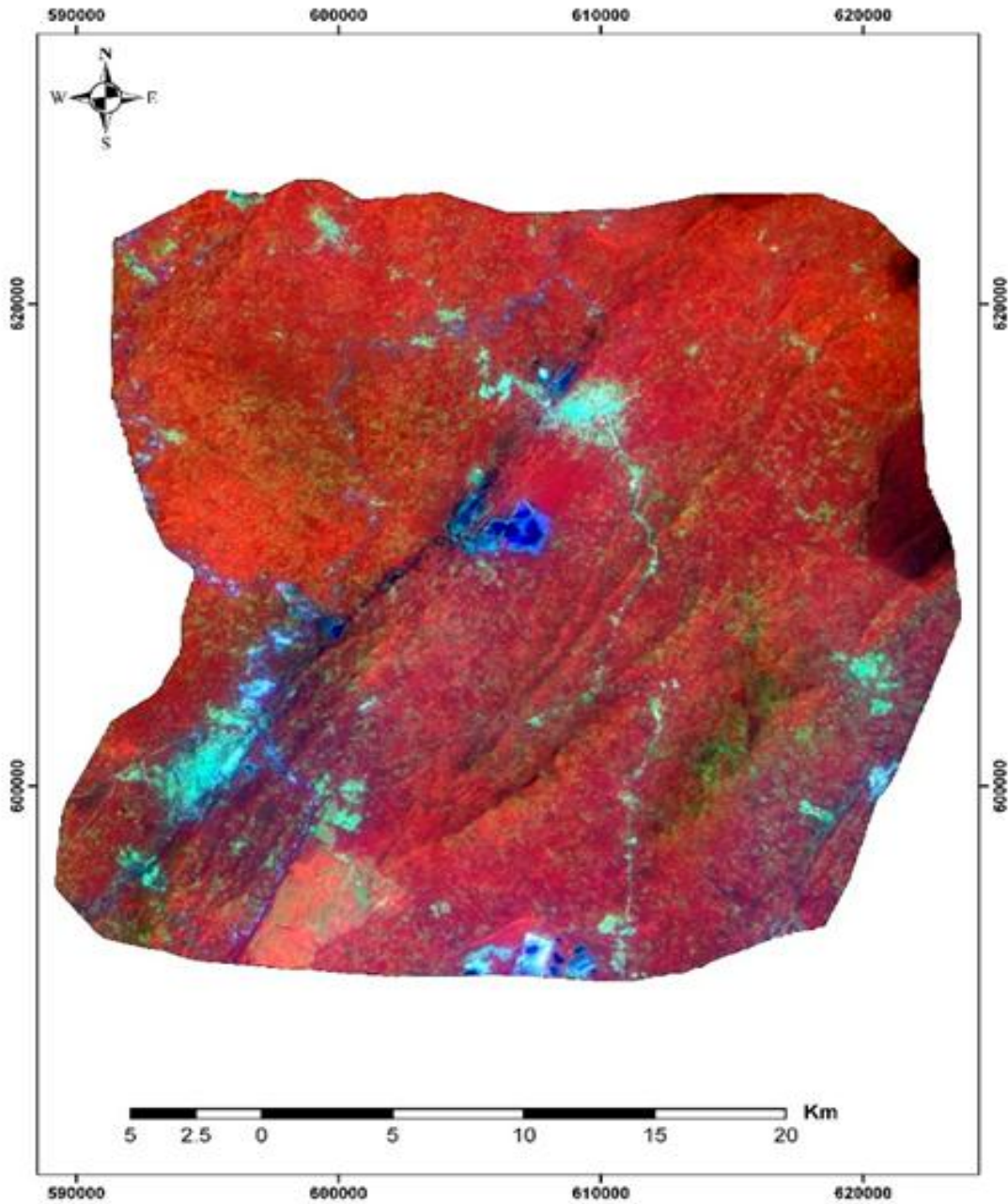


Figure-4. False colour composite Bands 5, 6, 7 in the study area.

3.2. Band Ratio

The band ratio 4/2 reveals areas that contain iron minerals and can be seen in bright tones in Figure 5. Iron oxide minerals have high absorption in TM band 2 and higher reflectance in TM band 4. Iron-stained hydrothermally rocks are shown by areas having higher Digital Numbers (DNs) as shown in the TM 4/2 ratio image Figure 5. The areas with high DN values are shown in bright tones and they relate to altered rocks. Band 6/5 ratio Figure 6 depicts areas with ferrous minerals due to the high reflectance of these minerals in this ratio (Gupta, 2003). Areas with high DN values are the bright tones in Figure 6 and depicts ferrous minerals alteration and hence correlate with altered rocks. Band ratio 7/5 detects clay mineralization in the study area. Areas with high DN values indicated by bright tones represent clay minerals alterations which correlate to altered rocks as shown in Figure 7. The clay minerals may be illite, montmorillonite or kaolinite. All these features have a high reflectance on band 6 and low reflectance in band 7 of the Landsat 8 image.

Band ratio 6/7 in Figure 8 shows altered rocks on the image with brighter pixels due to the reflectance features for the altered rocks in band 6 and absorption features in band 7 on Landsat 8 image. This ratio is considered the best ratio for mapping altered rocks (Ali and Pour, 2014). The combination of band ratios 4/2, 6/7 and 5 allows the recognition of outcrops as rose and brown, altered rocks as red areas, vegetation in light blue and water as black Figure 9. Kaufmann band ratio combinations using bands 7, 4, 3 and 5 in Landsat TM is equivalent to bands 7, 5, 4 and 6 in Landsat 8. Kaufmann band ratio was determined and it shows a good combination for geological determination. The Sabins band ratio 7/4, 6/3, 5/7 was also tested and it revealed a good geological purpose. From the final image Figure 10, black indicates water bodies, dark green indicates vegetation, light green indicates clay rich rocks and red indicates mineral rocks-iron oxides (Sabins, 1999; Abubakar *et al.*, 2014). The combination of band ratio 7/5, 5/4, 6/7 gives an image which where red represents minerals containing iron, green represents vegetated zones and blue represents OH/H₂O-, SO₄- or CO bearing minerals (Kaufmann, 1988; Abubakar *et al.*, 2014) displayed in Figure 11.

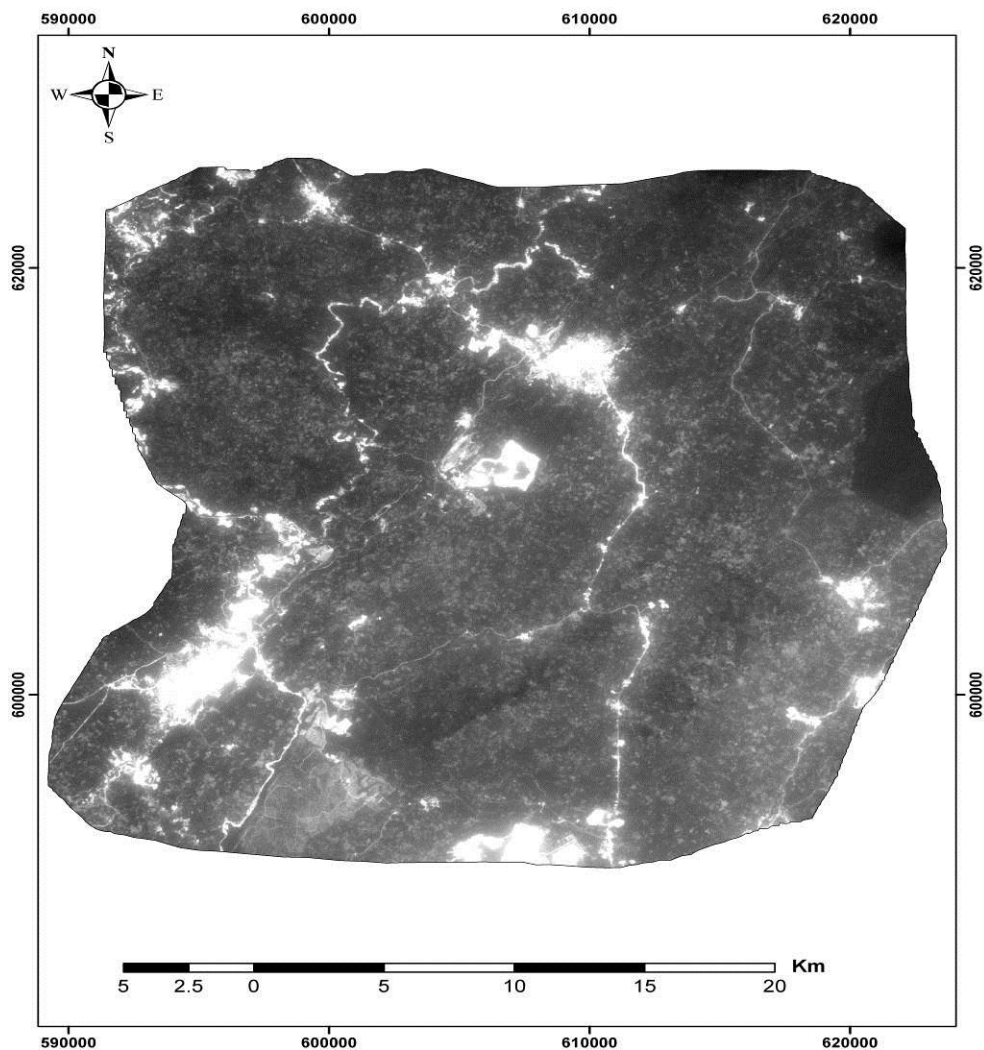


Figure-5. Landsat 8 band ratio 4/2 image. of the study area.

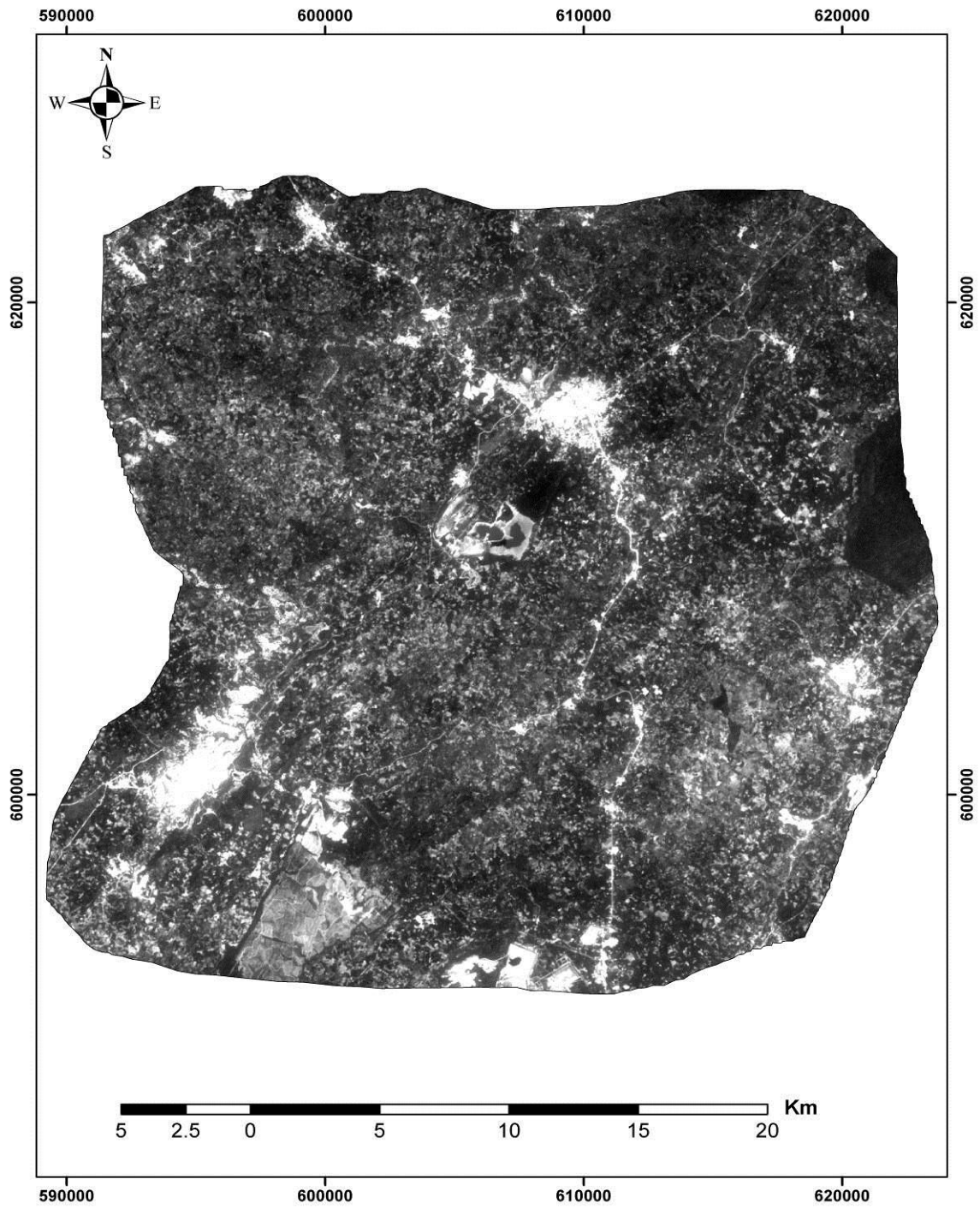


Figure-6. Landsat 8 band ratio 6/5 image of the study area.

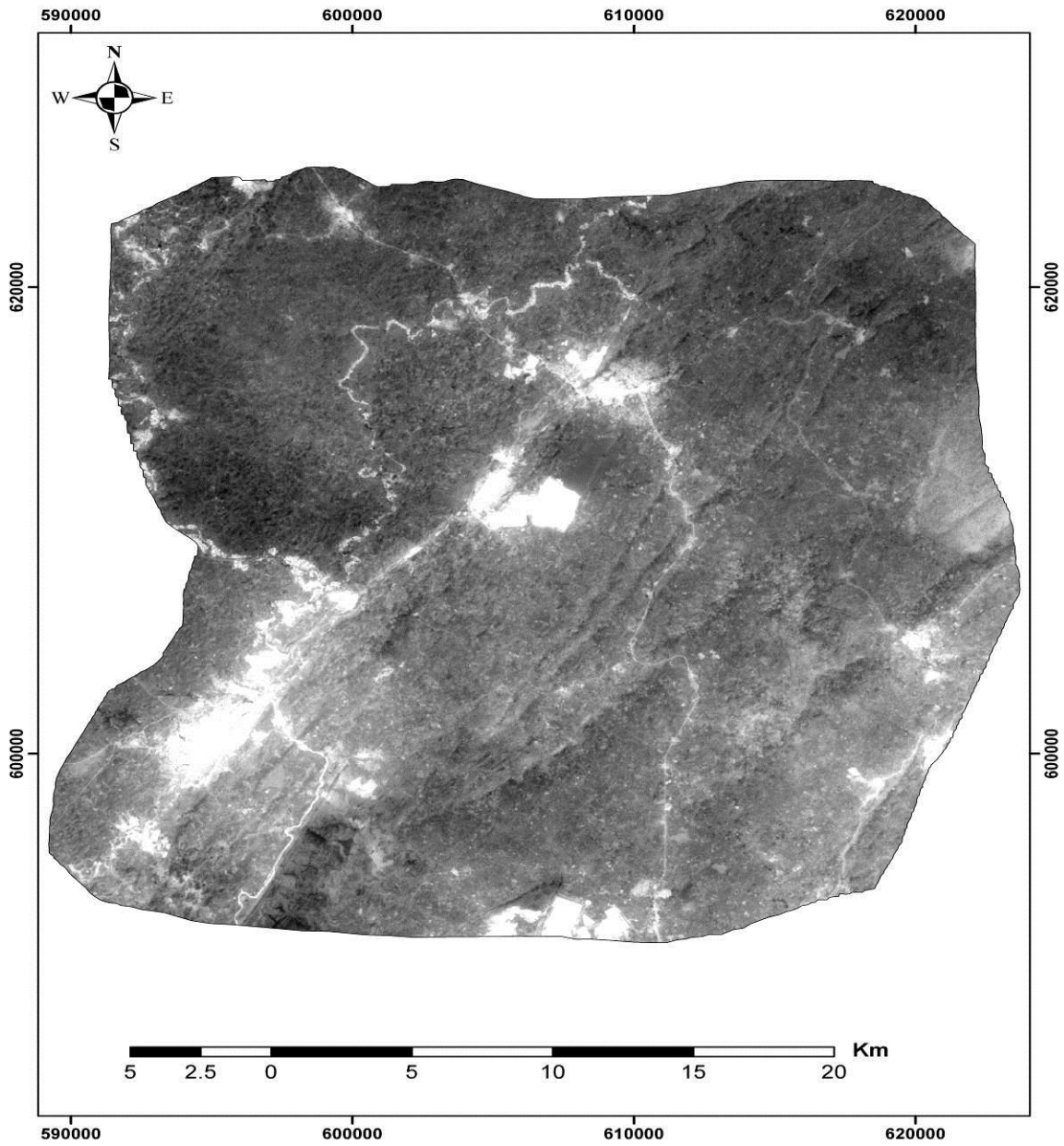


Figure-7. Landsat 8 band ratio (7/5) image of the study area.

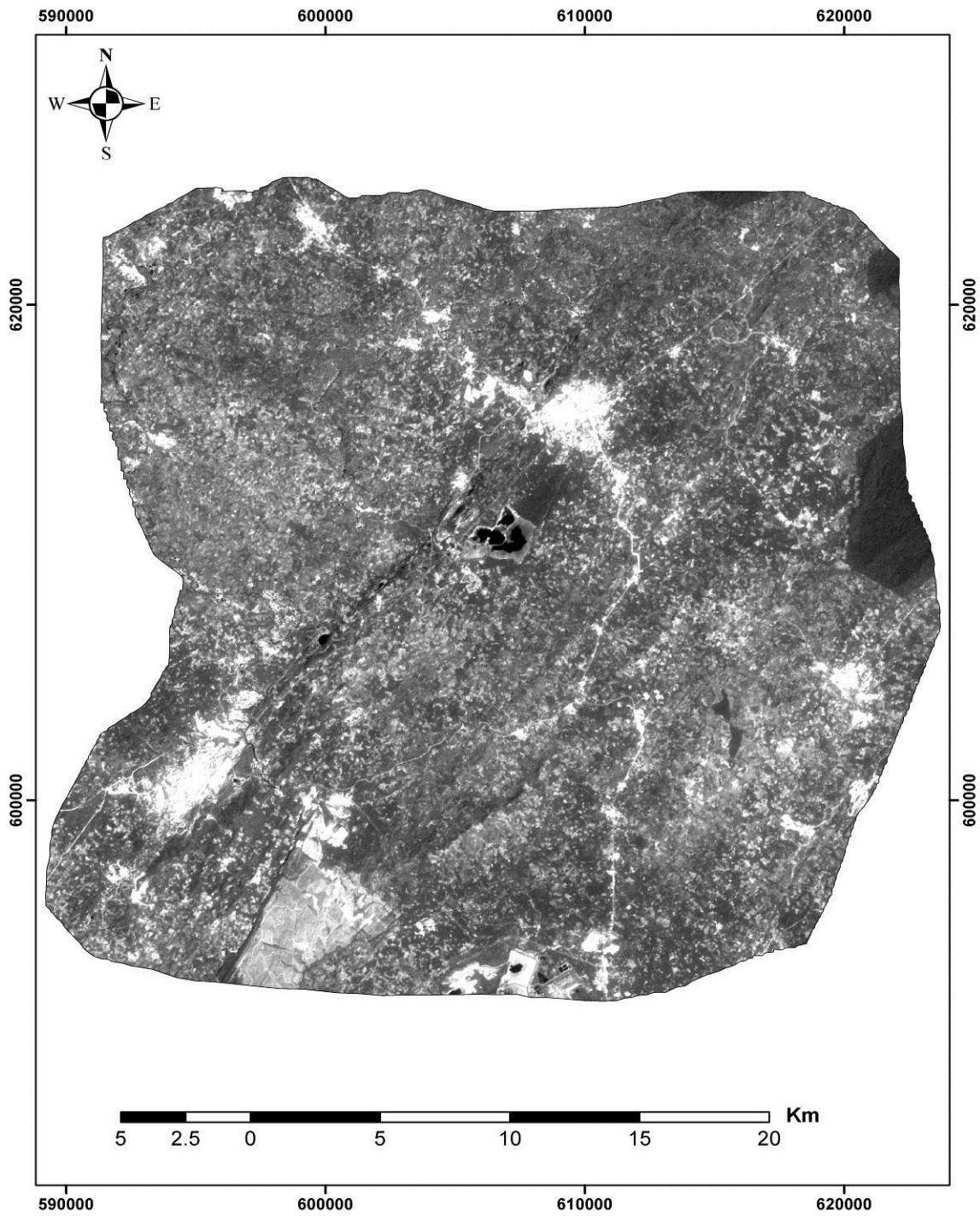


Figure-8. Landsat 8 band ratio (6/7) image of the study area.

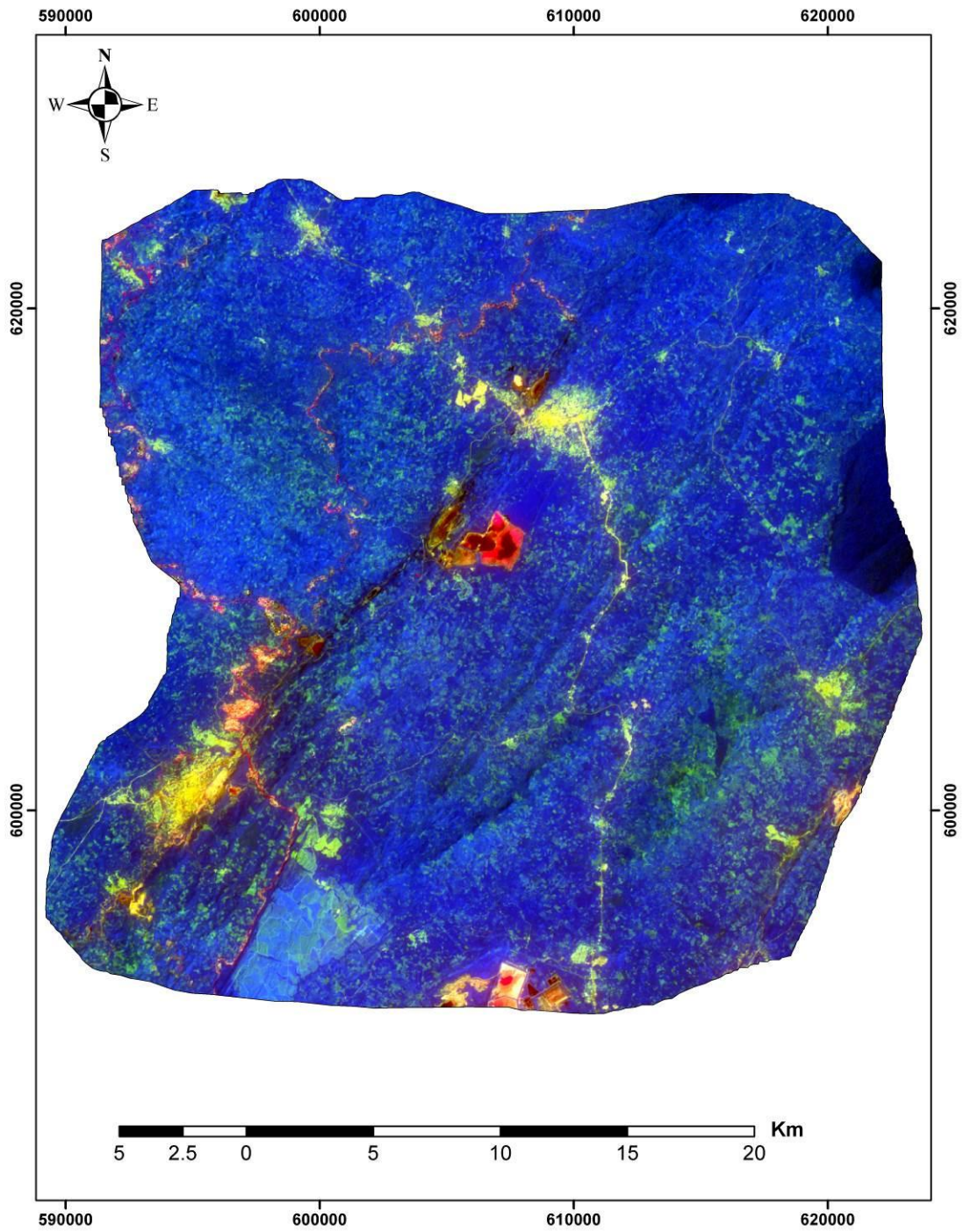


Figure-9. Colour composite of landsat 8 band ratio in RGB sequence:4/2 ,6/7 showing vegetation, outcrop and altered rocks in the study area.

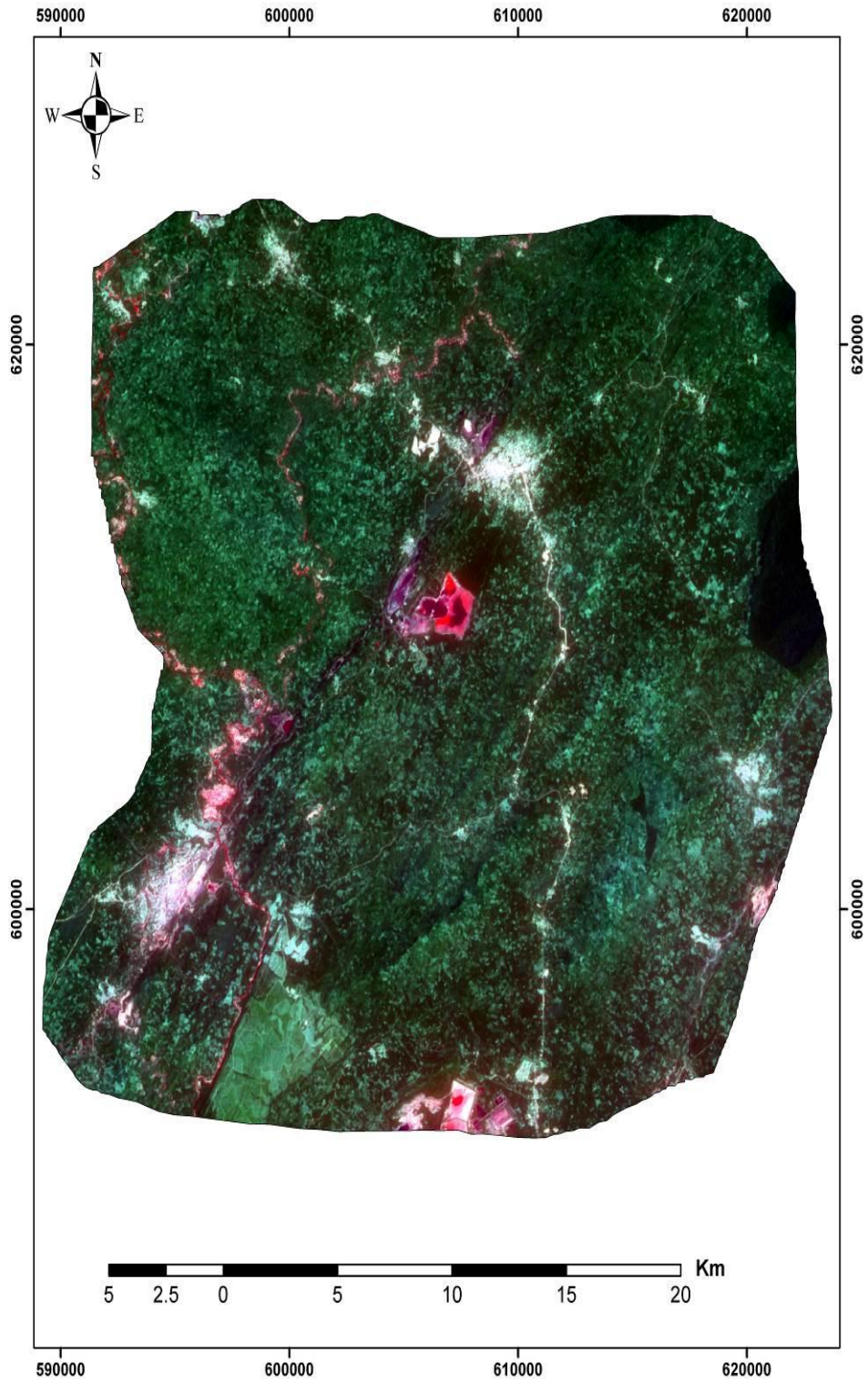


Figure-10. Sabin's ratio image (4/2, 6/7, 6/5) showing vegetation, outcrop and hydrothermal alterations in the study area.

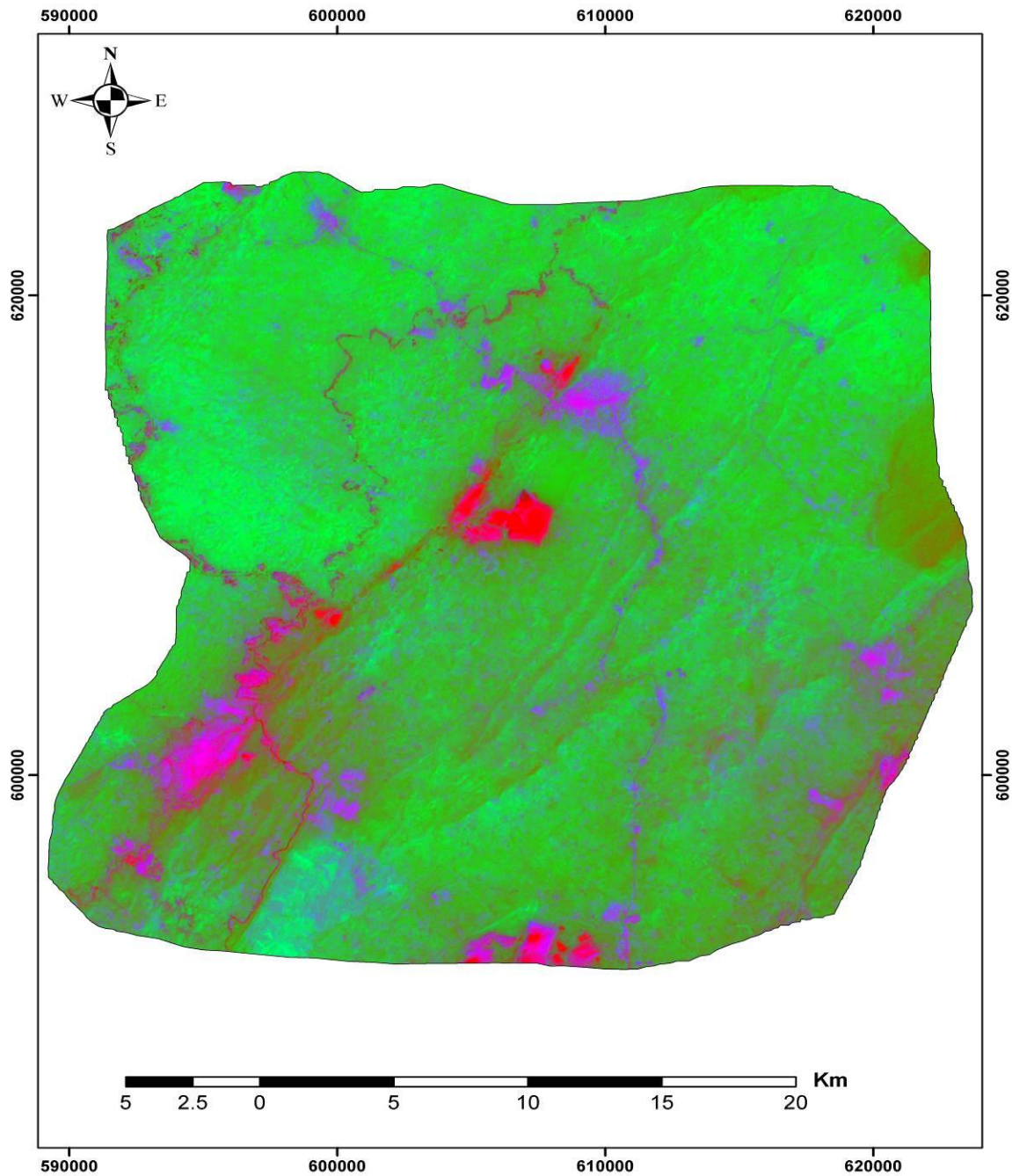


Figure-11. Kaufmann ratio image (7/5, 5/4, 6/7) showing vegetation, outcrop and hydrothermal alterations in the study area.

3.3. Principal Component Analysis and Crosta Technique

Firstly, the Principal Component Analysis was applied to the six Landsat 8 bands (2, 3,4,5,6, and 7). The technique was executed on two sets of band combination; 2456 and 2567 to map iron oxide and hydroxyl minerals respectively. The PCA eigenvector values are shown in tables below. PCA values for all bands is displayed in table 1. PC1 contains the highest amount (75.9%) of the total variance of the six bands and it gives information mainly on albedo and topography, it decreases till it reaches (0.1%) for PC 7. PC2 represent 14.6% of the total data variance and PC3 contain 8.0%. The first three high order principal components (PC1, PC2 and PC3) of input spectral bands gave more than 98% of the spectral information.

In Table 2 in Table 1, PC1 corresponds to the albedo image with 66.0% of data variance. PC2 indicates very high vegetated areas and are the dark pixels with a percentage of variance 21.5%. PC3 describes the contrast

between SWIR bands and visible/NIR bands. PC4 show negative eigenvector loading for band 7 (-0.75926) and positive eigenvector loading for band 6 (0.160409). Hence, hydroxyl bearing minerals are mapped as dark grey to black in the PC4 as shown in Figure 13. Hydroxyl-bearing minerals have reflectance features of 1.55-1.75 μm (band 6) and absorption of 2.1-2.4μm (band 7). PC4 highlights hydroxyl bearing minerals as dark grey to black pixels as shown in Figure 13. Clay minerals have absorption in band 7 and reflection in band 6.

PC1 corresponds to the albedo image with 66.9% of variance data Table 3. PC2 with 21.4% of variance represents the vegetated areas as darker pixels. PC3 represent the contrast of SWIR band between the visible and NIR bands. PC4 shows negative eigenvector loadings for band 2(-0.54278) and positive eigenvector loadings for band 4 (0.785618). Iron oxides minerals have absorption features and low reflectance of 0.45-0.51 μm in band 2 and reflectance features and low absorption of 0.64-0.67 μm in band 4. These two bands have higher loadings in PC analysis, and the pixels with more abundance of iron oxides minerals can be identified as bright pixels in PC4 image Figure 12.

Table-1. Principal component analysis of bands (2,3,4, 5, 6, 7).

Bands	PC1	PC2	PC3	PC4	PC5	PC6
Band2	0.439021	-0.06792	0.415927	-0.74209	0.095784	-0.2642
Band3	0.459153	-0.10998	0.210331	0.079218	-0.38578	0.76009
Band4	0.463945	0.000401	-0.01311	0.407753	-0.52491	-0.5855
Band5	0.20495	-0.95197	0.186454	0.098211	-0.01643	-0.0841
Band6	0.357922	-0.27526	-0.85131	-0.24668	0.089355	0.05059
Band7	0.459437	-0.03581	0.151983	0.454173	0.747137	0.0071
STD	2.1337	0.9345	0.69146	0.2522	0.1568	0.08744
Percentage Explined	75.8788	14.55592	7.968513	1.059668	0.409718	0.127429

Table-2. Principal component analysis of bands 2, 5, 6, 7 for hydroxyl minerals.

Bands	PC1	PC2	PC3	PC4
Band2	0.56626	0.105688	-0.52386	0.627491
Band5	0.3034	0.925537	-0.21742	-0.06357
Band6	0.48254	0.35364	0.785086	0.160409
Band7	0.59534	0.084565	-0.24888	-0.75926
STD	1.62476	0.926625	0.669874	0.229781
Percentage Explined	65.9959	21.46587	11.21828	1.319983

Table-3. Principal component analysis of bands 2,4,5,6 for iron oxide minerals.

Bands	PC1	PC2	PC3	PC4
Band2	0.55069	-0.10921	0.624665	-0.54278
Band4	0.59818	-0.0656	0.14382	0.785618
Band5	0.3125	-0.91599	0.220559	0.121081
Band6	0.49119	-0.38044	-0.73516	-0.27118
STD	1.63631	0.924687	0.647695	0.218926
Percentage Explined	66.9379	21.37616	10.48771	1.198209

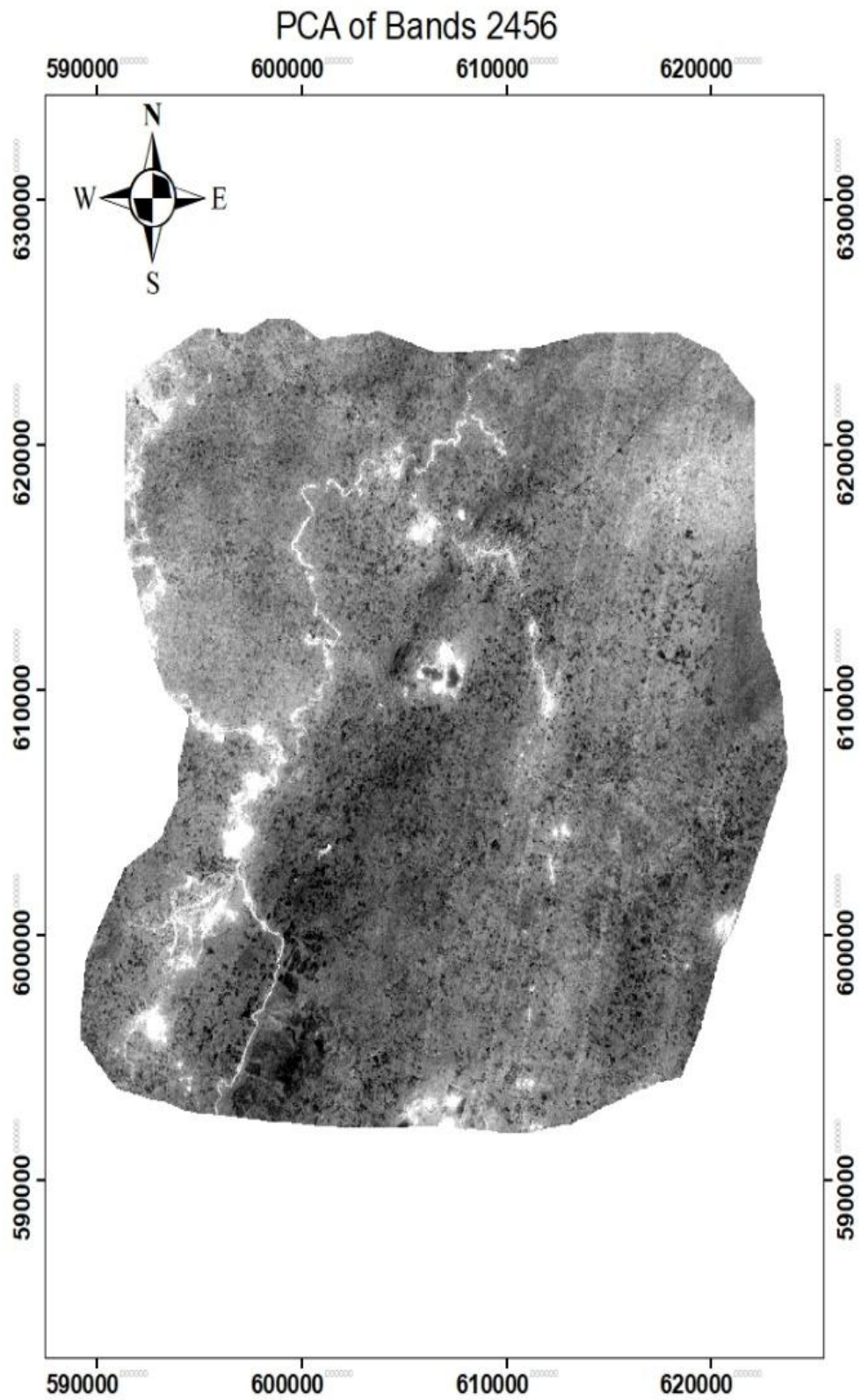


Figure-12. Showing Principal Component image from Landsat 8 data of iron oxide bearing minerals (PC4) as bright pixels.

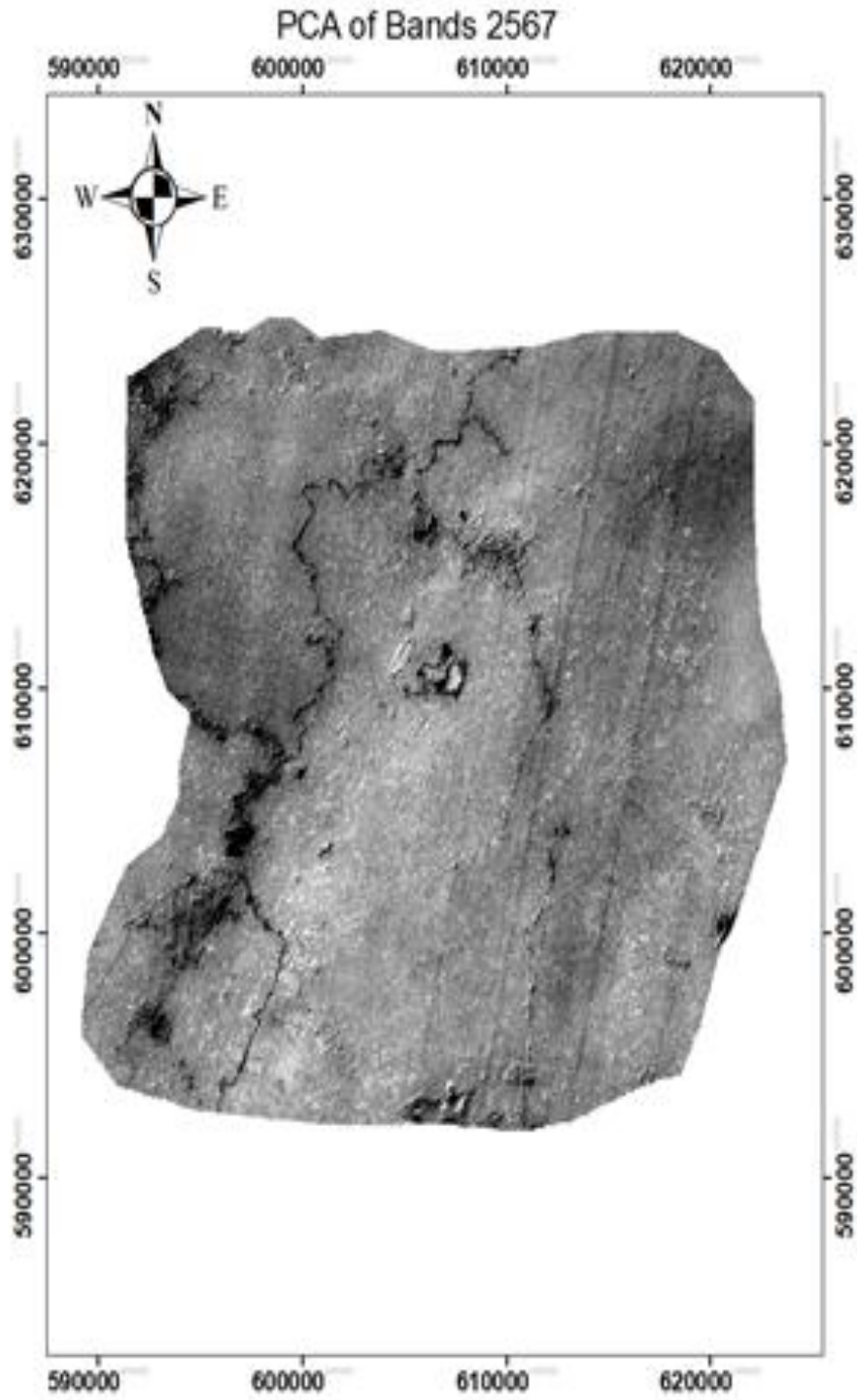


Figure-13. Showing Principal Component image from Landsat 8 data for hydroxyl minerals (PC4) as bright pixels.

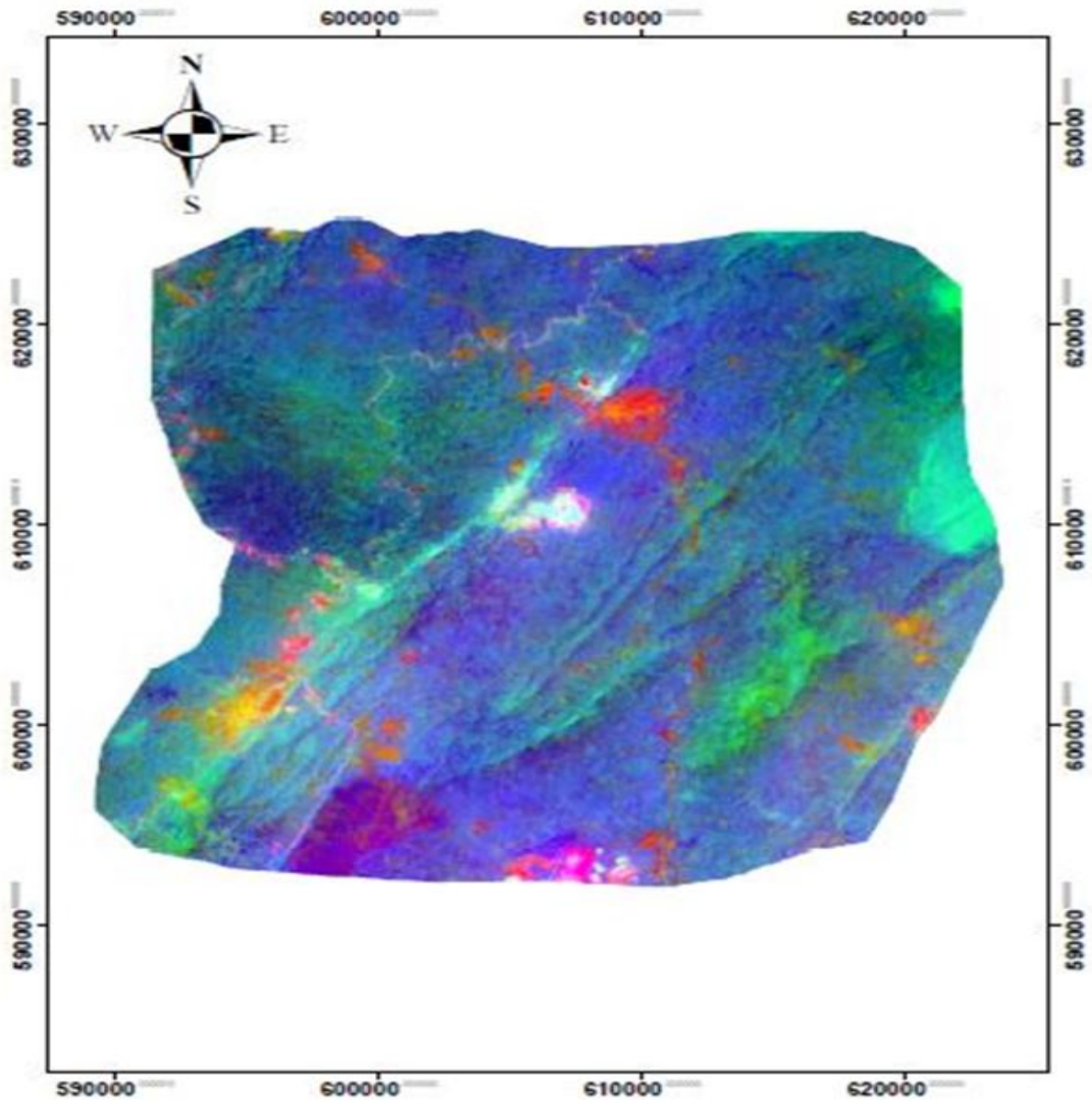


Figure-14. Colour composite of Principal Component 1,2,3 . Green-yellow colours represent granite outcrops, vegetation in green-blue, water as light blue and metasediments as blue.

Crosta technique was used to produce an image showing pixels with concentration in both iron oxide and hydroxyl minerals by merging iron oxide and hydroxyl bearing minerals images. Colour composite of the images corresponding to hydroxyl bearing minerals, the sum of both hydroxyl and iron oxide minerals, and iron oxide minerals are presented in RGB to permit the identification of alteration zones. Bright reddish to yellow agree with areas argillaceous than iron stained; bright cyan to bluish zones are more iron stained than argilized (Loughlin, 1991; Da Cunha Frutuoso, 2015) as shown in Figure 15.

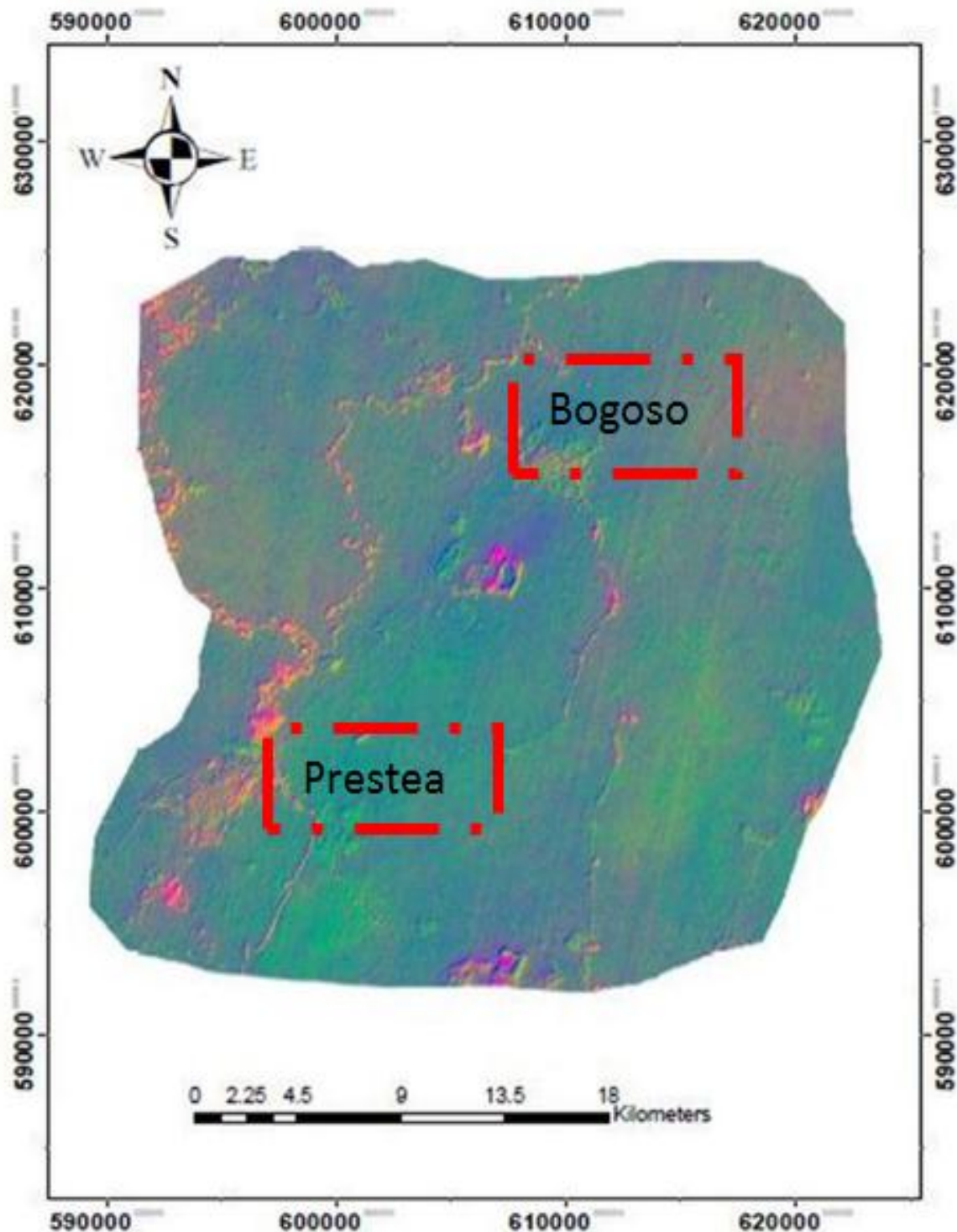


Figure-15. Colour composite of the images using hydroxyl bearing minerals ,the sum of both hydroxyl and iron oxide minerals and iron oxide minerals in RGB showing hydrothermal alteration areas.

4. DISCUSSIONS

Three band combinations, spectral ratioing and PCA were used in order to spectrally improve the reaction of iron-oxide, hydroxyl and clay minerals which signify to hydrothermal zones in Prestea Huni Valley district as shown in Figure 13 and 15. Iron oxides and clay minerals associated to hydrothermal alteration have been located using this approach. Band ratio technique applied on Landsat-8 data demonstrated to be acceptable for highlighting iron oxides and clay minerals at Bogoso and Prestea as shown in Figure 5,6,7 and 8. Band ratio 4/2 detects iron oxides mainly related to the rock types in Prestea and Bogoso areas, and also iron oxides below vegetation in the

study area. These minerals may be hematite, jarosite and goethite alterations and are formed by the oxidation of sulphide minerals (pyrite, chalcopyrite) within the rock units in the area. The presence of these mineral alterations as shown in [Figure 5](#) correlates with the presence of pyrites and chalcopyrite within the rock units in the area. These alteration minerals may have spatial relation with gold mineralization within the area. Areas with these alterations falls within the Bogoso concession where gold is mined as observed during the ground verification exercise and also with the local geology of the area. Further evidence is revealed within the northern part of the study area where Bogoso mine is located, which is characterized by gently dipping mineralized quartz vein stockworks and disseminated auriferous pyrite and arsenopyrite forming broad zones in the vicinity of the faulting zones. Smaller zones of disseminated sulfide mineralization coincide with areas where bedding and/or foliation in the adjacent Birimian sedimentary rocks is strongly discordant with the adjacent mineralized fault ([Allibone et al., 2002](#)).

Allibone added that, lower grade sulfide mineralization, commonly containing 2 to 10 g/t gold, is generally associated with disseminated arsenopyrite and/or pyrite in the graphitic mylonite fault rocks and the undeformed adjacent wall rocks (example ([Leube et al., 1990](#); [Milési et al., 1991](#))). These style of mineralization within the area also conforms to the two dominant types of shear zone-related mineralization which have been described from deposits hosted by the Birimian sedimentary rocks in Ghana. However, the principal association of gold within the Prestea and Bogoso gold districts are with arsenopyrite and arsenian pyrite. His studies depict that higher grade mineralization commonly containing >10 g/t free gold is generally hosted by quartz lodes localized in brittle fractures along controlling faults (examples ([Appiah, 1991](#); [Allibone et al., 2002](#))). According to Allibone, these higher grade lenses contain conspicuous arsenopyrite but completely absent in unmineralized lenses and this characteristic mineralization feature is very common in the prestea district than the Bogoso area.

The result of the Band ratio $7/5$ produced an acceptable index for highlighting of clay minerals. Clay minerals indicate the presence of silicate rocks which easily weather to release their clay components due to its low resistance to weathering. The clay minerals in this studies are suspected to be illite, montmorillonite or kaolinite. All these features have a high reflectance on band 6 and low reflectance in band 7 of the Landsat 8 image. Clay minerals was not adequately mapped in some portions due to the presence of thick vegetation within the study area. Sedimentary rocks, such as mudstone, shale, claystone and litharenite sandstone, contain large amounts of detrital clays such as montmorillonite, illite and kaolinite; these can be mistakenly be mapped as hydrothermally altered clay minerals. According to [Knepper \(1989;2010\)](#) the TM band ratio $7/5$ highlights carbonate minerals (calcite and dolomite), Fe-OH bearing minerals (epidote) and Mg-OH bearing phyllosilicate minerals (chlorite, talc and serpentine). In this opinion, the area with bright tone in [Figure 7](#) may not only be clay minerals but also carbonate minerals, chlorites, epidote, talc and serpentine. This conforms to the findings of ([Allibone et al., 2002](#)) on the Bogoso concession where gold is largely confined to the graphitic mylonite, which defines the fault zones, and imbricated slices of carbonate-altered rocks.

From principal component analysis ; PC1 gave positive eigenvalue loadings which makes distinguishing materials with spectral signature very difficult ([Jensen, 2005](#)). However, PC4 (Fig 6a) contains spectral information showing the iron-oxide bearing minerals in the study area which is significantly more than the percentage distinguished by utilizing band ratio of $4/2$. This is due to the fact that PCA rejects the impact of vegetation signature interference ([Ruiz-Armenta and Prol-Ledesma, 1998](#)). From [Figure 12](#) it can be seen that the iron-oxide materials formed little bunches within the study area. The style of gold mineralization within the area is structurally controlled and the graphitic mylonite and wall rock styles are similar to the sulphide mineralization at the Ashanti mine and other prominent mines within the belt such as Golden Star at Prestea ([Oberthür et al., 1998](#)). Both the PC4 [Figure 13](#) and band ratio [Figure 7](#) demonstrates a huge concentration of hydroxyl bearing minerals likely due to sericitisation during the alteration process. Indeed, in spite of the fact that the various band ratio colour composite in RGB shows the spatial distribution of hydrothermal alterations [Figure 9,10](#) and [11](#), it

overstated the degree of mineralization by representing unmineralized rock-outcrop and/or uncovered surface as hydrothermal alteration zones. This may be due to the impact of vegetation obstructions and the inability for some band ratio combination to distinguished between lithologies having same spectral signatures with the actual mineral deposits and also weathering of minerals to various part of the study area. Figure 15 shows hydrothermal alteration on satellite image conforming with Botwe *et al.* (2018) findings within the study area. Hydrothermal alteration on satellite image conforming with Botwe *et al.* (2018) findings within the study area. Hydrothermal deposits are formed when hot aqueous solutions containing minerals are deposited in weak zones and fissures. These fluids alters the materials they meet on their way and changes their color, chemical and mineralogical compositions. The fluids finally depositions its content and the minerals precipitates to form metaliferous deposits when are found in economic quantities. Mineral deposits from hydrothermal processes form economic reserves when they are concentrated in veins, and other cavities in lode forms or disseminated. Minerals such as quartz, pyrite, arsenopyrite are commonly associated with metalliferous minerals in lodes and they show alterations signatures in areas and have direct associations with mineralization. Same as the one acquired from the geology of the study area.

5. CONCLUSIONS AND RECOMMENDATIONS

The principal focus of this study was to conduct an investigation utilizing Landsat 8 and Remote sensing and GIS strategies to map various alteration in Prestea Huni valley District. Utilizing various alteration mapping techniques on the Landsat image in the study area, we found that the colour composite and band ratio approaches demonstrated their proficiencies to characterize the areas of clay mineral alterations, iron oxides minerals, vegetation and hydrothermal alteration. PCA presented the Fe oxides and hydroxyl altered minerals in the study area clearly. Consequently, it is reasonably clear that all these approaches are quite effective to map hydrothermal alteration using Landsat-8 OLI images and would be a very useful tool form exploration activities in the study area. These alterations correspond spatially with major gold mining sites in the study area and the signatures revealed during the studies conforms to the current signatures employed by the active mines in the area and also the general gold bearing zones within the Birimian sedimentary units of Ghana. The relationship demonstrated between the hydrothermal alteration map and major gold mining sites give an indication that, this method is suitable for the mapping of target areas in mineral exploration. However, the outcomes from the RS strategies of Landsat 8 image demonstrated the capacity of the data in mapping hydrothermal alteration zones at regional scale.

Funding: This work was supported by the African Union Commission.

Competing Interests: The authors declare that they have no competing interests.

Acknowledgement: All authors contributed equally to the conception and design of the study.

REFERENCES

- Abhary, A. and H. Hassani, 2016. Mapping hydrothermal mineral deposits using PCA and BR methods in Baft 1: 100000 Geological sheet, Iran. Ratio, 7(5): 6.
- Abubakar, A.J., M. Mazlan Hashim and A.B. Pour, 2014. Using landsat 8 (OLI) remote sensing data to map lithology and mineralogy for geothermal resource exploration. Geoscience and Digital Earth Centre (Geo-DEC), Research Institute for Sustainability and Environment (RISE), Universiti Teknologi Malaysia (UTM), 81310 UTM Skudai, Johor Bahru, Malaysia. Available from <http://a-a-r-s.org/acrs/index.php/acrs/acrs-overview/proceedings-1?view=publicationandtask=showandid=2488> [Accessed 1/02/2018].
- Abuzied, S.M., S.K. Ibrahim, M.F. Kaiser and T.A. Seleem, 2016. Application of remote sensing and spatial data integrations for mapping porphyry copper zones in Nuweiba area, Egypt. International Journal of Signal Processing Systems, 4(2): 102-108.

- Alimohammadi, M., S. Alirezaei and D.J. Kontak, 2015. Application of aster data for exploration of porphyry copper deposits: A case study of Daraloo–Sarmeshk area, southern part of the Kerman copper belt, Iran. *Ore Geology Reviews*, 70: 290-304. Available at: <https://doi.org/10.1016/j.oregeorev.2015.04.010>.
- Allibone, A., J. Teasdale, G. Cameron, M. Etheridge, P. Uttley, A. Soboh, J. Appiah-Kubi, A. Adanu, R. Arthur and J. Mamphey, 2002. Timing and structural controls on gold mineralization at the bogoso gold mine, Ghana, West Africa. *Economic Geology*, 97(5): 949-969. Available at: <https://doi.org/10.2113/97.5.949>.
- Amer, R., T. Kusky and A. Ghulam, 2010. Lithological mapping in the central Eastern Desert of Egypt using ASTER data. *Journal of African Earth Sciences*, 56(2-3): 75-82. Available at: <https://doi.org/10.1016/j.jafrearsci.2009.06.004>.
- Appiah, H., 1991. Geology and mine exploration trends of Prestea goldfields, Ghana. *Journal of African Earth Sciences (and the Middle East)*, 13(2): 235-241. Available at: [https://doi.org/10.1016/0899-5362\(91\)90008-m](https://doi.org/10.1016/0899-5362(91)90008-m).
- Botwe, T., E.O. Jnr, A.K. Kwaw and A.A. Omitogun, 2018. Hydrothermal alteration mapping using remote sensing and gis at the prestea concession of golden star bogoso/prestea ltd, Ghana. *International Journal of Engineering Science*, 8(1): 15898-15902. [Accessed 2/3/2018].
- Chavez, P., S.C. Sides and J.A. Anderson, 1991. Comparison of three different methods to merge multiresolution and multispectral data- Landsat TM and SPOT panchromatic. *Photogrammetric Engineering and Remote Sensing*, 57(3): 295-303.
- Crosta, A., C. De Souza Filho, F. Azevedo and C. Brodie, 2003. Targeting key alteration minerals in epithermal deposits in Patagonia, Argentina, using aster imagery and principal component analysis. *International Journal of Remote Sensing*, 24(21): 4233-4240. Available at: <https://doi.org/10.1080/0143116031000152291>.
- Da Cunha Frutuoso, R.M., 2015. Mapping hydrothermal gold mineralization using landsat 8 data. A Case of Study in Chaves License, Portugal.
- Dehnavi, A.G., R. Sarikhani and D. Nagaraju, 2010. Image processing and analysis of mapping alteration zones in environmental research, East of Kurdistan, Iran. *World Applied Sciences Journal*, 11(3): 278-283. Available at: <https://doi.org/10.12980/jclm.4.2016j6-50>.
- Gad, S. and T. Kusky, 2007. Aster spectral ratioing for lithological mapping in the Arabian–Nubian shield, the Neoproterozoic Wadi Kid area, Sinai, Egypt. *Gondwana Research*, 11(3): 326-335. Available at: <https://doi.org/10.1016/j.gr.2006.02.010>.
- Goetz, A.F., 2009. Three decades of hyperspectral remote sensing of the earth: A personal view. *Remote Sensing of Environment*, 113: S5-S16. Available at: <https://doi.org/10.1016/j.rse.2007.12.014>.
- Goetz, A.F., L.C. Rowan and M.J. Kingston, 1982. Mineral identification from orbit: Initial results from the shuttle multispectral infrared radiometer. *Science*, 218(4576): 1020-1024. Available at: <https://doi.org/10.1126/science.218.4576.1020>.
- Griffis, R.J., 1998. Explanatory notes-geological interpretation of geophysical data from Southwestern Ghana. Accra: Mineral Commission. pp: 51.
- Griffis, R.J., K. Barning, F.L. Agezo and F.K. Akosah, 2002. Gold deposits of Ghana. Ghana: Minerals commissions. Pp: 432.
- Jensen, J.R., 2005. *Introductory digital image processing: A remote sensing perspective*. Upper Saddle River, NJ: Pearson Prentice Hall.
- Jensen, J.R. and K. Lulla, 1987. *Introductory digital image processing: A remote sensing perspective*. 2(1): 65-65. Available at: <https://doi.org/10.1080/10106048709354084>.
- Kaufmann, H., 1988. Concepts, processing and results. *International Journal of Remote Sensing*, 9(10-11): 1639-1658. Available at: <https://doi.org/10.1080/01431168808954966>.
- Kesse, G.O., 1985. *The rock and mineral resources of Ghana*. Rotterdam, Netherlands: AA Balkema, .
- Knepper, D., 1989;2010. Mapping hydrothermal alteration with landsat thematic mapper data. *Mineral Deposits of North America*, 1: 13-21. Available at: <https://doi.org/10.1029/ft182p0013>.

- Kruse, F.A., S.L. Perry and A. Caballero, 2002. Integrated multispectral and hyperspectral mineral mapping, Los Menucos, Rio Negro, Argentina, Part II: EO-1 Hyperion/AVIRIS comparisons and landsat TM/ASTER extensions. In Proc. 11th JPL Airborne Geoscience Workshop. Jet Propulsion Laboratory.
- Kuma, J., Y.U. Kim, D. Boamah and I. Sakamoto, 2010. Gold Potential of the Ashanti Belt of Ghana. *Journal of the School of Marine Science and Technology, Tokai University*, 8(3): 25-39.
- Kwang, C., E.O. Jnr and A. Duker, 2014. Application of remote sensing and geographic information systems for gold potential mapping in Birim North District of Eastern Region of Ghana. *International Journal of Remote Sensing Applications*, 4(1): 48-55. Available at: <https://doi.org/10.14355/ijrsa.2014.0401.05>.
- Leube, A., W. Hirdes, R. Mauer and G.O. Kesse, 1990. The early proterozoic birimian supergroup of Ghana and some aspects of its associated gold mineralization. *Precambrian Research*, 46(1-2): 139-165. Available at: [https://doi.org/10.1016/0301-9268\(90\)90070-7](https://doi.org/10.1016/0301-9268(90)90070-7).
- Lillesand, T.M., R.W. Kiefer and J. Chipman, 2000. *Remote sensing and image analysis*. New York: John Wiley and Sons.
- Loughlin, W., 1991. Principal component analysis for alteration mapping. *Photogrammetric Engineering and Remote Sensing*, 57(9): 1163-1169.
- Masoumi, F., T. Eslamkish, M. Honarmand and A.A. Abkar, 2017. A comparative study of landsat-7 and landsat-8 data using image processing methods for hydrothermal alteration mapping. *Resource Geology*, 67(1): 72-88. Available at: <https://doi.org/10.1111/rge.12117>.
- Mia, B. and Y. Fujimitsu, 2012. Mapping hydrothermal altered mineral deposits using Landsat 7 ETM+ image in and around Kuju volcano, Kyushu, Japan. *Journal of Earth System Science*, 121(4): 1049-1057. Available at: <https://doi.org/10.1007/s12040-012-0211-9>.
- Milési, J., P. Ledru, P. Ankrah, V. Johan, E. Marcoux and C. Vinchon, 1991. The metallogenic relationship between birimian and tarkwaian gold deposits in Ghana. *Mineralium Deposita*, 26(3): 228-238. Available at: <https://doi.org/10.1007/bf00209263>.
- MLGRD, 2006. Western region (prestea-huni valley district).
- Mshiu, E.E., C. Gläßer and G. Borg, 2015. Identification of hydrothermal paleofluid pathways, the pathfinders in the exploration of mineral deposits: A case study from the sukumaland greenstone belt, Lake Victoria Gold Field, Tanzania. *Advances in Space Research*, 55(4): 1117-1133. Available at: <https://doi.org/10.1016/j.asr.2014.11.024>.
- Nouri, R., M. Jafari, M. Arain and F. Feizi, 2012. Hydrothermal alteration zones identification based on remote sensing data in the Mahin Area, West of Qazvin Province, Iran. *World Academy of Science, Engineering and Technology, International Journal of Environmental, Chemical, Ecological, Geological and Geophysical Engineering*, 6(7): 382-385.
- Oberthür, T., U. Vetter, D.W. Davis and J.A. Amanor, 1998. Age constraints on gold mineralization and Paleoproterozoic crustal evolution in the Ashanti belt of southern Ghana. *Precambrian Research*, 89(3-4): 129-143.
- Oduro, 2011. Prestea Huni-Valley District Assembly website. Available from www.ghanadistricts.com/districts [Accessed 12/08/2018].
- Pour, A.B. and M. Hashim, 2014. Hydrothermal alteration mapping using landsat-8 data, Sar Cheshmeh copper mining district, SE Iran. *Journal of Taibah University for Science*.
- Pour, A.B., M. Hashim, J.K. Hong and Y. Park, 2017. Lithological and alteration mineral mapping in poorly exposed lithologies using landsat-8 and aster satellite data: North-eastern Graham Land, Antarctic Peninsula. *Ore Geology Reviews*.
- Rajesh, H., 2004. Application of remote sensing and GIS in mineral resource mapping—An overview. *Journal of mineralogical and Petrological Sciences*, 99(3): 83-103. Available at: <https://doi.org/10.2465/jmps.99.83>.
- Ranjbar, H., M. Honarmand and Z. Moezifar, 2004. Application of the Crosta technique for porphyry copper alteration mapping, using ETM+ data in the southern part of the Iranian volcanic sedimentary belt. *Journal of Asian Earth Sciences*, 24(2): 237-243. Available at: <https://doi.org/10.1016/j.jseaes.2003.11.001>.

- Ruiz-Armenta, J.R. and R.M. Prol-Ledesma, 1998. Techniques for enhancing the spectral response of hydrothermal alteration minerals in Thematic Mapper images of Central Mexico. *International Journal of Remote Sensing*, 19(10): 1981-2000. Available at: 10.1080/014311698215108.
- Sabins, F.F., 1999. Remote sensing for mineral exploration. *Ore Geology Reviews*, 14(3-4): 157-183.
- Sadiya, T.B., O. Ibrahim, T.F. Asma, V. Mamfe, C.J. Nsofor, A.S. Oyewmi and M.S. Ozigis, 2014. Mineral detection and mapping using band ratioing and crosta technique in Bwari Area Council, Abuja Nigeria. *International Journal of Scientific and Engineering Research*, 5(12): 1100-1108.
- Van der Meer, F.D., H.M. Van der Werff, F.J. Van Ruitenbeek, C.A. Hecker, W.H. Bakker, M.F. Noomen, M. Van Der Meijde, E.J.M. Carranza, J.B. De Smeth and T. Woldai, 2012. Multi-and hyperspectral geologic remote sensing: A review. *International Journal of Applied Earth Observation and Geoinformation*, 14(1): 112-128.

Views and opinions expressed in this article are the views and opinions of the author(s), International Journal of Geography and Geology shall not be responsible or answerable for any loss, damage or liability etc. caused in relation to/arising out of the use of the content.